Backstepping control for a class of coupled hyperbolic-parabolic PDE systems*

Mohammad Ghousein, Emmanuel Witrant

***Abstract*— In this work, we consider the boundary stabilization of a linear diffusion equation coupled with a linear transport equation. This type of hyperbolic-parabolic partial differential equations (PDEs) coupling arises in many biological, chemical and thermal systems. The two equations are coupled inside the domain and at the boundary. The in-domain coupling architecture is considered from both sides i.e. an advection source term driven by the transport PDE and a Volterra integral source term driven by the parabolic PDE. Using a backstepping method, we derive two feedback control laws and we give sufficient conditions for the exponential stability of the coupled system in the L^2 norm. Controller gains are calculated by solving hyperbolic-parabolic kernel equations arising from the backstepping transformations. The theoretical results are illustrated by numerical simulations.**

I. INTRODUCTION

Partial differential equations (PDEs) can model many interesting physical processes. They are infinite dimensional systems that evolve not only in time but also in space. Examples of such systems can be found in multiple areas, such as fluid systems, population models, transport systems, biological reactors and many others. In this paper, we address an infinite dimensional system that involves two distinct classes of PDEs, namely hyperbolic and parabolic.

Coupled parabolic-hyperbolic systems naturally appear in many physical domains, such as predator-prey population models, biological chemotaxis and EUV lithography. It is important to note that many real processes that are modeled by hyperbolic equations (such as gas flow in pipelines [1], multiphase flow [2], heat exchanger networks [3], and many more) include a diffusive behavior that is neglected under specific hypotheses. A clear example regarding this property is the thermal heat exchanger tube, where heat is transfered from one fluid to another through a wall interface in which diffusion takes place. Under certain conditions related to the thermodynamic characteristics of the fluid and of the wall, the diffusion property cannot be neglected and the mathematical model involves a coupling between two different classes of PDEs.

The control of partial differential equations of the same class is widely investigated in the literature. Several results exist on the boundary control of hyperbolic systems [4], [5], [6], and also of parabolic systems [7], [8]. However, the boundary control of mixed hyperbolic-parabolic PDEs is less investigated by the community. In [9], the authors design a backstepping controller to stabilize a heat equation with arbitrarily long input delay. The system is viewed as a diffusion equation coupled with a transport equation just at the boundary (no interior coupling). In a more recent work [10], the authors solve the problem of stabilizing the same system as in [9] but considering a unidirectional Volterra coupling from diffusion to transport.

To the best of our knowledge, the contributions [9] and [10] are the only two works in the literature that address the problem of boundary stabilizing a mixed hyperbolic-parabolic system. In this context, we consider the control of almost the same class of systems investigated in [10]. The novelty in our work is to consider a bidirectional interior coupling between the two PDEs (i.e. an advection source term driven by the transport PDE and a Volterra integral source term driven by the parabolic PDE). This additional complexity in the model necessitates having two boundary control actuators instead of one.

The present paper also explores the applicability of the backstepping technique on systems of distinct families. For such class of systems, it is clear that the effectiveness of the backstepping method depends on the coupling topology as certain topologies can be quite difficult to tackle in theory. The coupling structure considered in this paper is a prime example on this difficulty.

The paper is organized as follows. The control problem formulation is described in Section II. The control design is presented in Section III. Section IV is dedicated to the exponential stability of the closed loop system. Finally, Section V illustrates the effectivness of the control design through simulations and some concluding remarks are given in Section VI.

II. PROBLEM DESCRIPTION

We consider the following class of mixed hyperbolic-parabolic system evolving in $\{(t,x) \mid t \geq 0, x \in [0,1]\}$:

$$v_t(x,t) = v_{xx}(x,t) + \lambda(x)v(x,t) + \sigma(x)u(x,t) \quad (1)$$

$$u_t(x,t) = u_x(x,t) + \int_0^x S(x,y)v(y,t)dy \quad (2)$$

$$v_x(0,t) = u(0,t) \quad (3)$$

$$v(1,t) = F_1(t) \quad (4)$$

$$u(1,t) = F_2(t) \quad (5)$$

where v and u are the coupled parabolic and hyperbolic states of the system, respectively. $S(x,y) \in C^\infty$ represents the coupling kernel from diffusion to transport, while $\sigma(x) \in$

*This work was sponsored within the ITEA3 European project, 15016 EMPHYSIS (Embedded systems with physical models in the production code software).

The authors are with Control Systems Department, GIPSA-lab, Grenoble, France. E-mails: {mohammad.ghousein, emmanuel.witrant}@gipsa-lab.fr

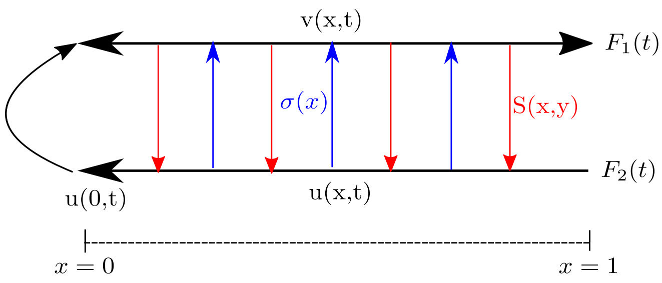

Fig. 1. Schematic diagram of the diffusive - advective system

$C^1[0,1]$ is the linear coupling from transport to diffusion. The reaction term $\lambda(x) \in C^1[0,1]$ is considered arbitrary. The outflow of the transport equation also drives the parabolic equation at the boundary $x=0$. Furthermore, the two coupled states are actuated using the two control laws $F_1(t)$ and $F_2(t)$ at $x=1$. A schematic representation of the plant can be found in Fig. 1.

III. Control Design

The overall objective is to design two feedback control laws $F_1(t)$ and $F_2(t)$ such that the exponential stability of system (1)-(5) is achieved in closed loop. It is important to note the two reasons which can cause system (1)-(5) to be unstable in open loop: one is the reaction term $\lambda(x) > 0$ which shifts the poles of the diffusion equation to the right hand plane. The second reason is the two couplings $S(x,y)$ and $\sigma(x)$ which, depending on their magnitude, may drive the system to unstability regardless of the value of $\lambda(x)$.
The control design is achieved with the following method. The diffusion equation (1) is first stabilized using the controller $F_1(t)$ to eliminate the instability caused by $\lambda(x)$. Afterwards, since the transport equation (2) can decay in finite time in case of no coupling from the diffusion equation, the idea is to decouple equation (2) using the controller $F_2(t)$, such that finite time decay is achieved for the transport PDE. The resulting system will be only diffusive and we give sufficient conditions that guarantees its stability in the L^2 norm (as we will show in the next sections). The previous procedure requires to have two backstepping transformations: Transformation 1 to obtain the controller $F_1(t)$ and Transformation 2 to obtain the controller $F_2(t)$.
We start by Transformation 1. Consider the following target system:
Target system 1:

$$
\begin{aligned}
z_t(x,t) = z_{xx}(x,t) - cz(x,t) + \sigma(x)u(x,t) + K(x,0)u(0,t) \\
- \int_0^x T(x,y)z(y,t)dy - \int_0^x K(x,y)\sigma(y)u(y,t)dy
\end{aligned} \tag{6}
$$

$$u_t(x,t) = u_x(x,t) + \int_0^x S_1(x,y)z(y,t)dy \tag{7}$$

$$z_x(0,t) = u(0,t) \tag{8}$$

$$z(1,t) = 0 \tag{9}$$

$$u(1,t) = F_2(t) \tag{10}$$

where $c > 0$ and $T(x,y)$ are two control design variables, and $S_1(x,y) = S(x,y) + \int_y^x S(x,\xi)L(\xi,y)d\xi$. The kernels $K(x,y)$ and $L(x,y)$ are to be defined later. To map system (1)-(5) to the target system (6)-(10), we consider the following backstepping transformation:
Transformation 1:

$$z(x,t) = v(x,t) - \int_0^x K(x,y)v(y,t)dy \tag{11}$$

$$v(x,t) = z(x,t) + \int_0^x L(x,y)z(y,t)dy \tag{12}$$

where the kernels $K(x,y)$ and $L(x,y)$ are the direct and inverse kernels, respectively, defined on the triangular domain $Ł_1 = \{(x,y), 0 \le y \le x \le 1\}$.

A. *Kernel equations for transformation 1*

Deriving (11) with respect to space and time, plugging into the target system 1 (equations (6)-(10)) yields the following system of kernel equations:

$$
\begin{aligned}
K_{xx}(x,y) - K_{yy}(x,y) = (c + \lambda(y))K(x,y) - T(x,y) \\
+ \int_y^x T(x,\xi)K(\xi,y)d\xi
\end{aligned} \tag{13}
$$

$$K_y(x,0) = 0 \tag{14}$$

$$K(x,x) = -\frac{1}{2}\int_0^x (\lambda(s) + c)ds \tag{15}$$

Following exactly the same procedure, one can calculate the kernel equations for the inverse transformation using (12). This gives the following set of equations:

$$
\begin{aligned}
L_{yy}(x,y) - L_{xx}(x,y) = (c + \lambda(x))L(x,y) + T(x,y) \\
+ \int_y^x L(x,\xi)T(\xi,y)d\xi
\end{aligned} \tag{16}
$$

$$L_y(x,0) = 0 \tag{17}$$

$$L(x,x) = -\frac{1}{2}\int_0^x (\lambda(s) + c)ds \tag{18}$$

It has been shown in [8] that the kernel equations (13)-(15) and (16)-(18) have a $C^2[Ł_1]$ unique solution. The control law $F_1(t)$ is calculated to ensure that $z(1,t) = 0$ and is given by:

$$F_1(t) = \int_0^1 K(1,y)v(y,t)dy \tag{19}$$

Target system 1 becomes a stable diffusion equation (with two free design variables c and $T(x,y)$ coupled with a transport equation. The objective of the controller $F_2(t)$ is then to decouple (7) from diffusion. By doing so the transport equation can achieve finite time stability. Consider the following target system:

Target system 2:

$$\eta_t(x,t) = \eta_{xx}(x,t) - c\eta(x,t) + \sigma(x)w(x,t) + K(x,0)w(0,t) + \int_0^1 C_1(x,y)\eta(y,t)dy + \int_0^x C_2(x,y)w(y,t)dy \tag{20}$$

$$w_t(x,t) = w_x(x,t) \tag{21}$$

$$\eta_x(0,t) = w(0,t) \tag{22}$$

$$\eta(1,t) = 0 \tag{23}$$

$$w(1,t) = 0 \tag{24}$$

where $C_1(x,y)$ and $C_2(x,y)$ are two feedforward couplings to be defined later. To map system (6)-(10) to system (20)-(24), we consider the following backstepping transformation:

Transformation 2:

$$\eta(x,t) = z(x,t) \tag{25}$$

$$w(x,t) = u(x,t) - \int_0^x P(x,y)u(y,t)dy - \int_0^1 M(x,y)z(y,t)dy \tag{26}$$

where the kernel $P(x,y)$ is defined on the triangular domain Ł$_1$ and $M(x,y)$ is defined on the rectangular domain Ł$_2 = \{(x,y), 0 \le x \le 1, 0 \le y \le 1\}$. We also postulate the inverse of transformation 2 as:

$$z(x,t) = \eta(x,t) \tag{27}$$

$$u(x,t) = w(x,t) + \int_0^x Q(x,y)w(y,t)dy + \int_0^1 R(x,y)\eta(y,t)dy \tag{28}$$

where $Q(x,y)$ and $R(x,y)$ are the inverse kernels defined on Ł$_1$ and Ł$_2$, respectively.

B. Kernel equations for transformation 2

Deriving (26) with respect to space and time, substituting into the target system 2 (equations (20)-(24)) yields the following system of kernel equations:

$$\begin{cases} \begin{cases} P_y(x,y) = -P_x(x,y) + \sigma(y)\Big(M(x,y) \\ -\int_y^x M(x,\xi)K(\xi,y)d\xi\Big) \end{cases} \\ P(x,0) = -M(x,0) + \int_0^x M(x,\xi)K(\xi,0)d\xi \end{cases} \tag{29}$$

$$\begin{cases} \begin{cases} M_x(x,y) = M_{yy}(x,y) - cM(x,y) \\ -S_1(x,y) + \int_y^x P(x,\xi)S_1(\xi,y)d\xi & \text{if } y \le x \\ -\int_y^x M(x,\xi)T(\xi,y)d\xi \end{cases} \\ M(x,y) = 0 & \text{if } y > x \\ M_y(x,0) = 0 \end{cases} \tag{30}$$

and yields the following equations for $C_1(x,y)$ and $C_2(x,y)$:

$$C_1(x,y) = \begin{cases} \sigma(x)M(x,y) - T(x,y) & \text{if } y \le x \\ +\int_y^x C_2(x,\xi)M(\xi,y)d\xi \\ 0 & \text{if } y > x \end{cases} \tag{31}$$

$$C_2(x,y) = \sigma(x)P(x,y) - \sigma(y)K(x,y) + \int_y^x C_2(x,\xi)P(\xi,y)d\xi \tag{32}$$

The control law $F_2(t)$ is calculated to ensure that $w(1,t) = 0$ and is given by:

$$\begin{aligned} F_2(t) &= \int_0^1 P(1,y)u(y,t)dy + \int_0^1 M(1,y)z(y,t)dy \\ &= \int_0^1 P(1,y)u(y,t)dy + \int_0^1 M_c(1,y)v(y,t)dy \end{aligned} \tag{33}$$

with $M_c(1,y) = M(1,y) - \int_y^1 M(1,\xi)K(\xi,y)d\xi$. In the same way, one can calculate the kernel equations for the inverse transformation using (28). This gives the following set of equations:

$$\begin{cases} \begin{cases} Q_y(x,y) = -Q_x(x,y) + \sigma(y)R(x,y) \\ +\int_y^x R(x,\xi)C_2(\xi,y)d\xi \end{cases} \\ Q(x,0) = -R(x,0) + \int_0^x R(x,\xi)K(\xi,0)d\xi \end{cases} \tag{34}$$

$$\begin{cases} \begin{cases} R_x(x,y) = R_{yy}(x,y) - cR(x,y) \\ -S_1(x,y) + \int_y^x R(x,\xi)C_1(\xi,y)d\xi \end{cases} & \text{if } y \le x \\ R(x,y) = 0 & \text{if } y > x \\ R_y(x,0) = 0 \end{cases} \tag{35}$$

Remark 1: Notice that the inverse equations (34)-(35) are similar to the direct transformation equations (29)-(30), except that $R(x,y)$ is uncoupled from $Q(x,y)$. As a result, the well-posedness of $R(x,y)$ implies the well-posedness of $Q(x,y)$, given the fact that $Q(x,y)$ is the first order transport equation.

C. Well-posedness of kernel equations for transformation 2

We start with the well-posedness of the direct transformation as the inverse will follow exactly in the same way. The transport equation (29) can be explicitly solved as a function of $M(x,y)$ using the method of characteristics:

$$\begin{aligned} P(x,y) = &-M(x-y,0) + \int_0^y \sigma(\xi)M(x-y+\xi,\xi)d\xi \\ &+ \int_0^{x-y} M(x-y,\xi)K(\xi,0)d\xi \\ &- \int_0^y \int_s^{x-y+s} \sigma(s)M(x-y+s,\xi)K(\xi,s)d\xi ds \end{aligned} \tag{36}$$

Then, the existence of $M(x,y)$ is sufficient to show that both $P(x,y)$ and $M(x,y)$ exist. Inserting (36) into (30), the $M(x,y)$ kernel equations become:

$$\begin{cases} \begin{cases} M_x(x,y) = M_{yy}(x,y) - cM(x,y) - S_1(x,y) \\ -\int_y^x M(x,\xi)T(\xi,y)d\xi + \int_y^x \Big(-M(x-\xi,0) \\ +\int_0^\xi \sigma(s)M(x-\xi+s,s)ds & \text{if } y \le x \\ +\int_0^{x-\xi} M(x-\xi,s)K(s,0)ds - \int_0^\xi \int_v^{x-\xi+v} \\ \sigma(v)M(x-\xi+v,s)K(s,v)dsdv\Big)S_1(\xi,y)d\xi \end{cases} \\ M(x,y) = 0 & \text{if } y > x \\ M_y(x,0) = 0 \end{cases} \tag{37}$$

The $M(x,y)$ PDE kernel equations (37) are nearly the same as the $l(x,y)$ kernel equations obtained by the authors in [10], except that $M(x,y)$ has a zero initial condition ($M(0,y)=0$, which gives $M(x,y)=0$ if $y>x$, whereas in [10], $l(0,y)\neq 0$). $M(x,y)$ also contains additional linear integral terms related to the coupling with the transport equation. To prove the existence of a weak solution, the idea is to first compute energy estimates of the solution. These estimates depend only on the initial conditions and the source terms. Afterwards, a Galerkin type argument can be used to prove the existence of solutions (see [11] for more details). We give only partial elements of the proof as the rest is the same as in [10]. We state the energy estimates result in the following lemma:

Lemma 1: Consider the $M(x,y)$ PDE system (37). There exist a function $F:\mathbb{R}^+\to\mathbb{R}^+$ such that:

$$\max_{s\in[0,x]}||M(s)||_{H^1}+||M||_{L^2([0,x],H^1)}\leq F(\bar{S}) \tag{38}$$

where $\bar{S}= ||S_1(x,y)||_{L^2([0,1],H^2[0,1])}$.

Proof: We define the H^1 norm in the y-direction as:

$$\begin{aligned}||M(x)||^2_{H^1[0,1]}&=\int_0^1 M^2(x,y)dy+\int_0^1 M_y^2(x,y)dy\\&=||M(x)||^2_{L^2[0,1]}+||M_y(x)||^2_{L^2[0,1]}\end{aligned} \tag{39}$$

Using (37), integration by parts, and applying Young's and Agmon's inequalities [7] we get:

$$\begin{aligned}\frac{d}{dx}||M(x)||^2_{L^2}\leq&\Bigg(-2c+\frac{1}{2}+\bar{T}+\bar{S}_1+\frac{1}{2}\Sigma\bar{S}_1+\frac{1}{2}\mathbb{K}\bar{S}_1\\&+\Sigma\mathbb{K}\bar{S}_1\Bigg)||M(x)||^2_{L^2}+\bar{S}_1^2+\frac{1}{2}\bar{T}||M(x)||^2_{H^1}\\&+\left(\bar{S}_1+\Sigma\bar{S}_1+\mathbb{K}\bar{S}_1+\Sigma\mathbb{K}\bar{S}_1\right)\max_{s\in[0,x]}||M(s)||^2_{H^1}\end{aligned} \tag{40}$$

where $\Sigma=||\sigma(x)||_{L^\infty[0,1]}$, $\bar{T}=||T(x,y)||_{L^2([0,1],H^2[0,1])}$ and $\mathbb{K}=||K(x,y)||_{L^\infty[Ł_1]}$. In the same way, using (37), one can derive the following bound on the derivative of $||M_y(x)||^2_{L^2[0,1]}$:

$$\begin{aligned}\frac{d}{dx}||M_y(x)||^2_{L^2}\leq&\Bigg(-2c+\frac{1}{2}+2\bar{T}+\frac{3}{2}\Sigma\bar{S}_1+\frac{3}{2}\mathbb{K}\bar{S}_1+2\Sigma\mathbb{K}\bar{S}_1\\&+2\bar{S}_1\Bigg)||M_y(x)||^2_{L^2}+\bar{S}_1^2+\frac{1}{2}\bar{T}||M(x)||^2_{H^1}\\&+\bar{T}||M(x)||^2_{L^2}\\&+2\left(\Sigma\bar{S}_1+\mathbb{K}\bar{S}_1+\Sigma\mathbb{K}\bar{S}_1+\bar{S}_1\right)\max_{s\in[0,x]}||M(s)||^2_{H^1}\end{aligned} \tag{41}$$

By adding (40) and (41), we get the following differential inequality in the H^1 norm of $M(x,y)$:

$$\begin{aligned}\frac{d}{dx}||M(x)||^2_{H^1}\leq&\Bigg(-2c+\frac{1}{2}+3\bar{T}+2\bar{S}_1+\frac{3}{2}\Sigma\bar{S}_1+\frac{3}{2}\mathbb{K}\bar{S}_1\\&+2\Sigma\mathbb{K}\bar{S}_1\Bigg)||M(x)||^2_{H^1}+2\bar{S}_1^2\\&+3\left(\Sigma\bar{S}_1+\mathbb{K}\bar{S}_1+\Sigma\mathbb{K}\bar{S}_1+\bar{S}_1\right)\max_{s\in[0,x]}||M(s)||^2_{H^1}\end{aligned} \tag{42}$$

We solve (42) by considering two seperate cases: increasing and decreasing cases (the constant case is obvious). Staring with the increasing case, we have that $\max_{s\in[0,x]}||M(s)||^2_{H^1}=|||M(x)||^2_{H^1}$, and (42) becomes:

$$\begin{aligned}\frac{d}{dx}||M(x)||^2_{H^1}\leq&\Bigg(-2c+\frac{1}{2}+3\bar{T}+5\bar{S}_1+\frac{9}{2}\Sigma\bar{S}_1\\&+\frac{9}{2}\mathbb{K}\bar{S}_1+5\Sigma\mathbb{K}\bar{S}_1\Bigg)||M(x)||^2_{H^1}+2\bar{S}_1^2\end{aligned} \tag{43}$$

Using the comparison principle, and recalling that $M(x,y)$ has zero initial condition $M(0,y)=0$, one can derive the following H^1 bound on $M(x,y)$:

$$\begin{aligned}||M(x)||^2_{H^1}\leq\int_0^x 2\bar{S}_1{}^2\exp\Bigg(\Bigg(&-2c+\frac{1}{2}+3\bar{T}+5\bar{S}_1+\frac{9}{2}\Sigma\bar{S}_1\\&+\frac{9}{2}\mathbb{K}\bar{S}_1+5\Sigma\mathbb{K}\bar{S}_1\Bigg)(x-z)\Bigg)dz\end{aligned} \tag{44}$$

On the other hand, and in a quite similar way, we note in the decreasing case that $\max_{s\in[0,x]}||M(s)||^2_{H^1}=|||M(0)||^2_{H^1}=0)$, and (42) becomes:

$$\begin{aligned}\frac{d}{dx}||M(x)||^2_{H^1}\leq&\Bigg(-2c+\frac{1}{2}+3\bar{T}+2\bar{S}_1+\frac{3}{2}\Sigma\bar{S}_1+\frac{3}{2}\mathbb{K}\bar{S}_1\\&+2\Sigma\mathbb{K}\bar{S}_1\Bigg)||M(x)||^2_{H^1}+2\bar{S}_1^2\end{aligned} \tag{45}$$

Following the same procedure, one can derive the following H^1 norm on $M(x,y)$:

$$\begin{aligned}||M(x)||^2_{H^1}\leq\int_0^x 2\bar{S}_1{}^2\exp\Bigg(\Bigg(&-2c+\frac{1}{2}+3\bar{T}+2\bar{S}_1+\frac{3}{2}\Sigma\bar{S}_1\\&+\frac{3}{2}\mathbb{K}\bar{S}_1+2\Sigma\mathbb{K}\bar{S}_1\Bigg)(x-z)\Bigg)dz\end{aligned} \tag{46}$$

By (44) and (46), one can find a mapping F such that (38) is fulfilled. ■

Theorem 1: The kernel PDE defined by (37) has a weak solution in $L^2([0,1],H^1[0,1])$.

Proof: Using a Galerkin construction of the solution and by applying Lemma 1, a weak solution is guaranteed to exist due to the energy estimate obtained in (38) (see [10] for more details). ■

In order to ensure the existence of a bounded solution for $C_1(x,y)$ and $C_2(x,y)$ in equations (31) and (32), we take the following assumption on the weak solution of $M(x,y)$ proved in Theorem 1.

Assumption 1: Assume that the weak solution $M(x,y)$ of the kernel PDE defined by (37) is bounded for all (x,y) in $Ł_2$.

The boundedness of $M(x,y)$ by assumption 1 implies the boundedness of $P(x,y)$ by (36). Since equation (32) is a Volterra equation in $C_2(x,y)$ with a bounded source $\sigma(x)P(x,y)-\sigma(y)K(x,y)$ and a bounded kernel $P(x,y)$, then $C_2(x,y)$ admits a bounded solution in $Ł_1$. As a result, $C_1(x,y)$ also admits a bounded solution in $Ł_2$ using (31).

IV. Stability of the closed loop system

We start by considering the exponential stability of the system (η, w). One can use Transformations 1 and 2 to conclude on the exponential stability of the (v,u) system. The target system 2 is in a cascade form: a finite-time ($t_F = 1s$) stable transport equation (w) which drives a diffusion equation (η). After t_F, the stability of (η) is directly related to the magnitude of the Fredholm integral variable $C_1(x,y)$. However, the magnitude of $C_1(x,y)$ can be modified through the two design control variables c and $T(x,y)$ embedded in $C_1(x,y)$ (see equation 31).

Theorem 2: For all $t > t_F = 1s$, the transport state $w \equiv 0$ for any initial condition $w(x,0) \in L^{\infty}[0,1]$. If there exist $\delta_1 > 0$ and two control variables $c > 0$ and $T(x,y)$ such that

$$-\frac{\pi^2}{4} - c + ||C_1||_{L^{\infty}[\text{Ł}_2]} \leq -\delta_1 \tag{47}$$

then the diffusive state (η) is L^2 stable for any initial condition $\eta(x,0) \in L^2[0,1]$.

Proof: It is obvious to see that $w \equiv 0$ after $t_F = 1s$ and it is indeed stable in the L^{∞} norm (see [12]), hence for $t > t_F$, target system 2 becomes:

$$\eta_t(x,t) = \eta_{xx}(x,t) - c\eta(x,t) + \int_0^1 C_1(x,y)\eta(y,t)dy \tag{48}$$

$$\eta_x(0,t) = 0 \quad \text{and} \quad \eta(1,t) = 0 \tag{49}$$

Now, we consider the following Lyapunov function:

$$V_1(t) = \frac{1}{2}\int_0^1 \eta^2(x,t)dx \tag{50}$$

Differentiating (50) with respect to time, using integration by parts and applying Wirtinger inequality [7], we have:

$$\dot{V}_1(t) \leq -(\frac{\pi^2}{4} + c)||\eta||_{L^2}^2 + \int_0^1\int_0^1 C_1(x,y)\xi(y,t)\xi(x,t)dydx \tag{51}$$

Then using Cauchy-Shwartz inequality [7] we have:

$$\dot{V}_1(t) \leq \int_0^1 \left(-\frac{\pi^2}{4} - c + ||C_1||_{L^{\infty}[\text{Ł}_2]} \right) \eta^2(x,t)dx \tag{52}$$

If (47) is satisfied, we have $\dot{V}_1(t) \leq -2\delta_1 V_1(t)$ which gives the exponential decay of $V_1(t)$ in the L^2 sense with a convergence rate $\gamma = -2\delta_1$ and concludes the proof of Theorem 2. ■

As the stability of the system (η, w) is proven in the L^2 sense after the time t_F, then using the boundedness and the invertibility of transformations 1 and 2, we can conclude that the initial system (v,u) is exponentially stable in the L^2 sense.

Remark 2: After the time $t_F = 1s$, the target system 2 is only diffusive and its stability depends on the magnitude of $C_1(x,y)$. It is useful to view $C_1(x,y)$ as a function of the parameters as $C_1(\lambda, \sigma, S, c, T)$. The parameter c is interpreted as a convergence rate parameter. If $c = 0$, the free variable $T(x,y)$ helps in finding δ_1 such that (47) is satisfied. Otherwise i.e. if $T(x,y) = 0$, the stability condition (47) will depend only on the magnitude of the system's parameters ($\lambda(x)$, $\sigma(x)$, $S(x,y)$). Since the dependency of $C_1(x,y)$ on c and $T(x,y)$ is extremely convoluted, we use a search algorithm to find the admissable values of c and $T(x,y)$ that satisfy (47) (as illustrated in Section V).

V. Simulation Results

The performance of the control architecture is evaluated on its ability to stabilize an unstable open loop system. We have performed simulations taking into consideration the two mentioned reasons for instability (see Section III) i.e. we choose $\lambda = 3 > \frac{\pi^2}{4}$, $\sigma(x) = 4$, $S(x,y) = 5e^{1-y}cos(x)$. As predicted from the chosen values of $(\lambda, \sigma(x), S(x,y))$, the plant is open loop unstable and this is confirmed by the response in Fig.2.

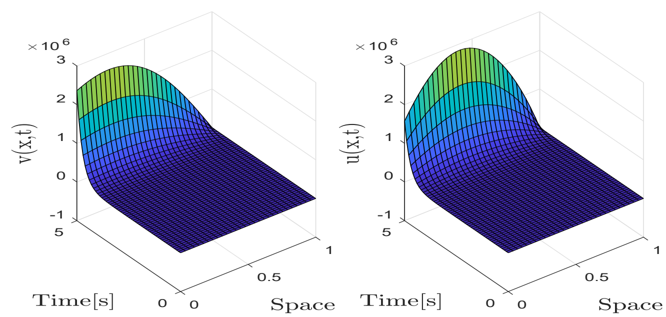

Fig. 2. The unstable system in open loop.

The second step is to calculate the two controllers $F_1(t)$ and $F_2(t)$ that stabilize the system. This requires solving offline the kernels $K(x,y)$, $L(x,y)$, $M(x,y)$ and $P(x,y)$ to obtain the controller gains. Two unknowns are required to solve the kernels: c and $T(x,y)$.

A. Calculation of c and T(x,y)

The two control variables c and $T(x,y)$ are principally calculated to ensure that inequality (47) is satisfied. We proceed in the following order:

- fix the variables c and δ_1 as the speed of convergence parameters;
- $T(x,y)$ is written using Legendre polynomials as follows, $\forall (x,y) \in \text{Ł}_1$:

$$T(x,y) = \sum_{p=0}^{N}\sum_{q=0}^{N} \alpha_{p,q} P_p(x) P_q(y) \tag{53}$$

  where $\alpha_{0,0}, \ldots, \alpha_{N,N}$ are some constant coefficients, $P_q(x)$ is the q^{th} order Legendre polynomial, N is the order of the Legendre polynomials;
- we write the kernels $K(x,y)$ and $L(x,y)$ in the integral form (see [8]), these equations are approximated using the left Rieman sum approximation. Afterwards, the $M(x,y)$ kernel is discretized and calculated using a finite differences scheme. The kernels $P(x,y)$, $C_2(x;y)$ and $C_1(x,y)$ are calculated using the integral equations (36), (32) and (31) respectively;

- using a Monte-Carlo simulation method, we solve

$$\max_{\alpha_{p,q}} |C_1| < \frac{\pi^2}{4} + c - \delta_1 \tag{54}$$

  to find the values of the constants $\alpha_{p,q}$. We start the search algorithm with zero degree of freedom polynomials i.e. $T(x,y) = cst$. The level of complexity can be increased to include more degrees of freedom in case of difficulties in finding solutions.

For the values of the system parameters mentioned above, inequality (54) was solved for $c = 1$, $\delta_1 = 0.85$ and a constant value for $T(x,y) = T = 1.67$. The controller gains are given on Fig. 3. Actuating the system with the two feedback control laws $F_1(t)$, $F_2(t)$ shown in Fig.4 quickly drives the system exponentially to zero after exhibiting some transient behavior due to the initial conditions, as shown by the closed loop response on Fig.5.

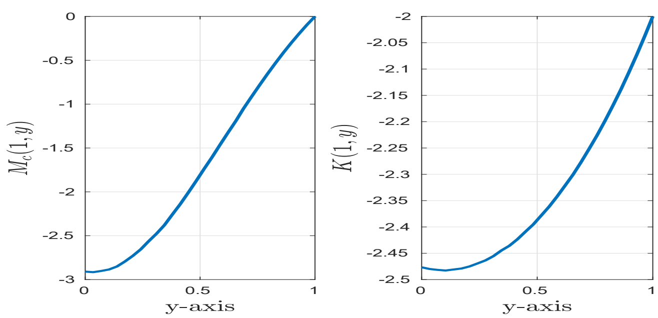

Fig. 3. The control gain kernels.

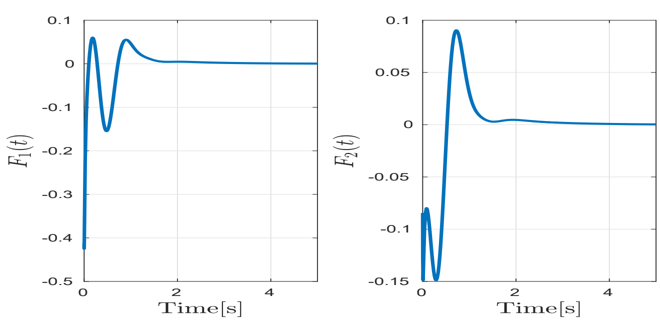

Fig. 4. The two controllers $F_1(t)$ and $F_2(t)$.

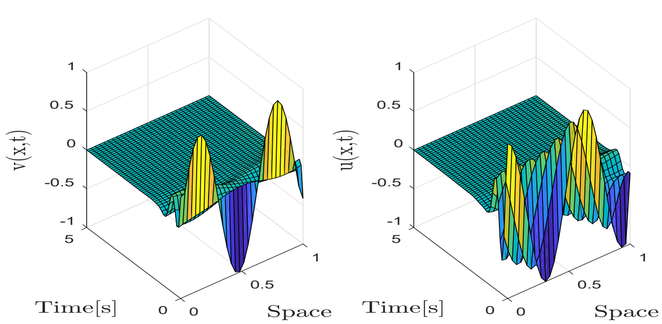

Fig. 5. The exponentially stable closed loop system.

VI. CONCLUSIONS

We have presented in this paper a boundary control architecture for a system of coupled hyperbolic-parabolic equations. The plant under consideration has couplings in both directions, i.e. from the hyperbolic side to the parabolic side and vice versa. The control design is based on using backstepping transformations to map the initial system into an exponentially stable target system. With a clever choice of the target systems, the resulting kernel equations were very similar to the ones obtained in previous control designs [9], [10] which makes the presented structure simple and familiar to implement. We have also illustrated the effectiveness of the boundary control on an unstable plant using numerical simulations.

The primary difficulty of using backstepping design on systems of mixed-classes is the different number of space derivatives corresponding to each family in the overall plant. It is well known that the backstepping method is very powerful when dealing with coupled systems of same class, but the topic of stabilizing different classes of coupled systems is still under research.

The class of systems investigated in the paper is a step towards other interesting hyperbolic-parabolic models resulting from various physical applications, that do not have an integral term in the advective flow (just reactive coupling). Such systems appear in refrigeration cycles and specially in heat exchanger networks. This adds more importance in studying to which extent we can apply the backstepping technique on mixed classes of hyperbolic-parabolic systems.

REFERENCES

[1] M. Gugat and M. Dick, "Time-delayed boundary feedback stabilization of the isothermal euler equations with friction," *Math. Control Relat. Fields*, vol. 1, no. 4, pp. 469–491, 2011.

[2] F. Di Meglio, "Dynamics and control of slugging in oil production," Ph.D. dissertation, École Nationale Supérieure des Mines de Paris, 2011.

[3] C.-Z. Xu and G. Sallet, "Exponential stability and transfer functions of processes governed by symmetric hyperbolic systems," *ESAIM: Control, Optimisation and Calculus of Variations*, vol. 7, pp. 421–442, 2002.

[4] G. Bastin and J.-M. Coron, *Stability and boundary stabilization of 1-d hyperbolic systems*. Springer, 2016, vol. 88.

[5] L. Hu, F. Di Meglio, R. Vazquez, and M. Krstic, "Control of homodirectional and general heterodirectional linear coupled hyperbolic PDEs," *IEEE Transactions on Automatic Control*, vol. 61, no. 11, pp. 3301–3314, 2016.

[6] F. Castillo, E. Witrant, C. Prieur, and L. Dugard, "Boundary observers for linear and quasi-linear hyperbolic systems with application to flow control," *Automatica*, vol. 49, no. 11, pp. 3180–3188, 2013.

[7] M. Krstic and A. Smyshlyaev, *Boundary control of PDEs: A course on backstepping designs*. SIAM, 2008, vol. 16.

[8] A. Smyshlyaev and M. Krstic, *Adaptive control of parabolic PDEs*. Princeton University Press, 2010.

[9] M. Krstic and A. Smyshlyaev, "Backstepping boundary control for first-order hyperbolic PDEs and application to systems with actuator and sensor delays," *Systems & Control Letters*, vol. 57, no. 9, pp. 750–758, 2008.

[10] S. Chen, R. Vazquez, and M. Krstic, "Backstepping control design for a coupled hyperbolic-parabolic mixed class PDE system," in *2017 IEEE 56th Annual Conference on Decision and Control (CDC)*. IEEE, 2017, pp. 664–669.

[11] L. C. Evans, "Partial differential equations," *Providence, RI*, 1998.

[12] M. Krstic, *Delay compensation for nonlinear, adaptive, and PDE systems*. Springer, 2009.